Journal of Biomolecular NMR, **25:** 243–248, 2003.
KLUWER/ESCOM

Extending the range of amide proton relaxation dispersion experiments in proteins using a constant-time relaxation-compensated CPMG approach

Rieko Ishima* & Dennis A. Torchia*
Molecular Structural Biology Unit, National Institute of Dental and Craniofacial Research, National Institutes of Health, Bethesda, MD 20892-4307, U.S.A.

Received 1 August 2002; Accepted 6 November 2002

Key words: chemical exchange, conformational change, NMR, CPMG, R_2

Abstract

Relaxation compensated constant-time Carr–Purcell–Meiboom–Gill relaxation dispersion experiments for amide protons are presented that detect μs-ms time-scale dynamics of protein backbone amide sites. Because of their ten-fold larger magnetogyric ratio, much shorter 180° pulses can be applied to ^{1}H than to ^{15}N spins; therefore, off-resonance effects are reduced and a wider range of effective rf fields can often be used in the case of ^{1}H experiments. Applications to [^{1}H-^{15}N]-ubiquitin and [^{1}H-^{15}N]-perdeuterated HIV-1 protease are discussed. In the case of ubiquitin, we present a pulse sequence that reduces artifacts that arise from homonuclear $^3J(H_N\text{-}H_\alpha)$ coupling. In the case of the protease, we show that relaxation dispersion of both ^{1}H and ^{15}N spins provides a more comprehensive picture of slow backbone dynamics than does the relaxation dispersion of either spin alone. We also compare the relative merits of ^{1}H versus ^{15}N transverse relaxation measurements and note the benefits of using a perdeuterated protein to measure the relaxation dispersion of both spin types.

Communication

Relaxation dispersion experiments, that measure the nuclear spin transverse relaxation rate, R_2, as a function of the effective rf field strength, are well suited to detect slow protein dynamics on the μs-ms time scale (Palmer et al., 2001). Recently, pulse sequences have been presented that measure relaxation dispersion of ^{15}N backbone amides, ^{13}C methyl groups, and ^{15}N side-chain NH_2 groups (Mulder et al., 2001, 2002; Skrynnikov et al., 2001; Tollinger et al., 2001). These sequences utilize a relaxation compensating element, rcINEPT (Loria et al., 1999), in conjunction with a constant-time CPMG period. This approach enables efficient measurement of R_2 over a wide range of effective rf fields.

Herein we present a pulse sequence (Figure 1) that detects relaxation dispersion of amide protons in proteins. The pulse sequence shown in Figure 1A is a straightforward modification of the constant-time ^{15}N relaxation dispersion experiment (Tollinger et al., 2001) in which two CPMG periods are separated by an rcINEPT element. The rcINEPT element converts H_y magnetization to H_xN_z magnetization resulting in relaxation compensation (Loria et al., 1999). When ^{15}N R_1 is ca. 10 times smaller than ^{1}H R_2, little error is introduced into an ^{1}H R_2 measurement if relaxation compensation is not used, provided that the effective rf field, ν_{CP}, is greater than ca. 100 Hz (where, $\nu_{CP} = \gamma B_{eff} = 1/4\tau_{CP}$, and $2\tau_{CP}$ is the time between the centers of CPMG refocusing pulses). However, this is not the case at smaller values of ν_{CP} and larger values of R_1/R_2.

In order to derive the amide proton relaxation profile, amide ^{1}H R_2 values at each value of ν_{CP} are determined from the ratios of two sets of signal intensities. One set of signal intensities is obtained from a reference spectrum, recorded without the CPMG periods depicted in Figure 1A. The other set of signal intensities is derived from a spectrum recorded using the pulse sequence in Figure 1A, with the value

*To whom correspondence should be addressed. E-mails: dtorchia@dir.nidcr.nih.gov; rishima@dir.nidcr.nih.gov

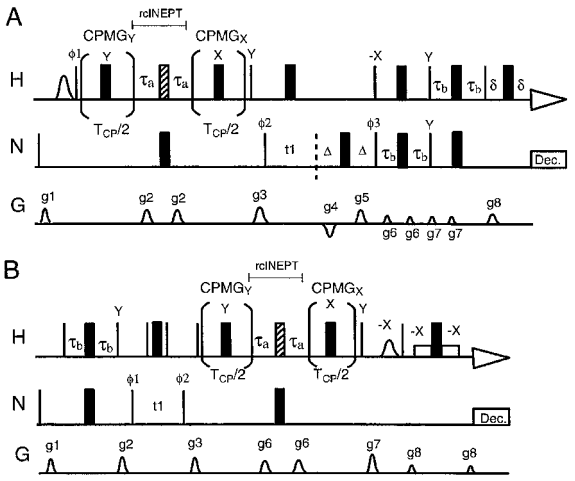

Figure 1. (A) Pulse scheme of the amide ^{1}H relaxation dispersion experiment used in the case of a protonated ubiquitin. Narrow (wide) bars correspond to 90° (180°) rf pulses applied with phase x, unless indicated otherwise. Non-rectangular rf and gradient pulses had the shape of the first lobe of a sine function. The shaped pulse at the start of the sequence is a 1 ms sine pulse that selectively excites water protons. A proton 180° rf pulse applied between the first and second CPMG periods, shown by a hatched bar, is either a composite rectangular pulse or 3 ms REBURP pulse (see details in the text). The total length of the two CPMG periods, T_{CP}, is 40 ms. Since a minimum of two 180° pulses is required in each CPMG period, the lowest effective field strength is 50 Hz. Values of delays are: $\tau_a = 2.7$ ms; $\tau_b = 2.25$ ms; $\Delta = 1.5$ ms; $\delta = 1$ ms. The phase cycle is $\phi1 = \{x, -x\}$, $\phi2 = \{y, y, -y, -y\}$,$\phi3 = \{x\}$, and $\phi_{receiver} = \{x, -x, -x, x\}$. Placing the CPMG periods before the t_1 evolution period allows quadrature detection in t_1 using the sensitivity enhancement approach (Kay et al., 1992; Palmer et al., 1991) where for each value of t_1 separate data sets are acquired for ($\phi3$, g4, g5) and ($\phi3+180°$, $-$g4, $-$g5). All gradients were applied along z with a maximum amplitude of 35 G cm^{-1}, except 28 G cm^{-1} for g_8. Gradient durations for g_1-g_8 were 0.8 ms, 0.6 ms, 2.4 ms, 0.92 ms, 0.92 ms, 0.6 ms, 0.5 ms and 0.23 ms, respectively. (B) The modified sequence, which reduces the proton transverse relaxation rate by placing the CPMG periods after the t_1 evolution period, was used to record spectra of perdeuterated HIV-1 protease. Open squares indicate rectangular 180° pulses of 2 ms. Data were acquired using $T_{cp} = 80$ ms, with ν_{CP} varied from 25 Hz to 2 kHz in an interleaved manner. The phase cycle is $\phi1 = \{x, -x\}$, $\phi2 = \{x, x, -x, -x\}$ and $\phi_{receiver} = \{x, -x, -x, x\}$. All gradients were applied along z with a maximum amplitude of 35 G/cm and durations of 0.8 ms, 1.0 ms, 1.0 ms, 0.6 ms, 2.3 ms, and 0.4 ms for g_1, g_2, g_3, g_6, g_7 and g_8, respectively. In both sequences, the phases of the $CPMG_x$ ($CPMG_y$) pulses are $-$x ($-$y) during the first (second) interleave cycles. All proton rectangular pulses had 90° pulse widths of 10 μs and 12.5 μs at 500 MHz and 800 MHz, respectively. Proton pulses are applied centered on the water resonance except from the beginning of the first CPMG period to the end of the second CPMG period, where the rf carrier position is set to 8.3 or 8.5 ppm. For each t_1 increment, axial peaks are shifted to the edge of the spectrum by inversion of $\phi2$ in concert with the receiver phase in both experiments (Marion et al., 1989).

of ν_{CP} determined by the number of CPMG refocusing pulses applied during T_{CP} (Mulder et al., 2001). An advantage of this two-point method of deriving R_2 is that correct values of chemical exchange relaxation rates are obtained from the relaxation profiles even when transverse relaxation due to other mechanisms (e.g., multi spin dipole-dipole interactions) is multi-exponential (Mulder et al., 2001).

Proton dispersion pulse sequences were tested using a ^{15}N uniformly labeled ubiquitin sample. In contrast to the analogous ^{15}N dispersion experiment, use of non-selective rectangular 180° refocusing pulses in the CPMG and rcINEPT periods resulted in spurious dispersion profiles for many amide sites in the protein. Examples of this behavior are shown in Figure 2A. The spurious dispersion is predicted by numerical simulations and occurs because the homonuclear $^{3}J(H_N\text{-}H_\alpha)$ coupling is active during the CPMG and rcINEPT periods. A similar artifact was found to affect the measurement of Leu C_δ methyl carbons, due to $^{3}J(C_\delta\text{-}C_\alpha)$ coupling (Mulder et al., 2002). In the latter case, the spurious dispersion was eliminated by application of 500 μs REBURP (Geen and Freeman, 1991) CPMG pulses that selectively refocused the C_δ magnetization. Unlike the Leu C_δ and C_α carbons whose separation is large compared with their chemical shift dispersions, the separation of the amide and α-protons is comparable to the chemical shift dispersion of each type of proton. This necessitates the use of a 3 ms REBURP pulse to selectively refocus the amide protons and at the same time not perturb the α-protons. The large duration of the REBURP pulse limits the maximum value of ν_{CP} to ca. 150 Hz. For this reason, we replaced only the non-selective rectangular ^{1}H 180° pulse in the rcINEPT period by a 3 ms REBURP pulse that selectively refocused amide proton magnetization. This pulse removed most of the spurious dispersion from the relaxation profiles of the amide residues, even those in β-strands which experience the largest $^{3}J(H_N\text{-}H_\alpha)$ couplings (Figure 2B).

A drawback of using the single REBURP pulse is that nearly all amide dispersion profiles show a small increase in R_2 as the effective field increases, Figure 2B. When there is no homonuclear coupling, each pair of CPMG pulses compensates nearly perfectly for small imperfections (e.g., arising from off resonance) in the 180° pulses. (Carr and Purcell, 1954; Meiboom and Gill, 1958). In contrast, when homonuclear $^{3}J(H_N\text{-}H_\alpha)$ is active, $I_{zN}I_{z\alpha}$ coherence accumulates as the number of the applied 180° pulses increases. Therefore, as ν_{CP} (i.e., the number of 180° pulses)

increases, magnetization is irreversibly lost due to a combination of resonance offset (Ross et al., 1997) and $^3J(H_N\text{-}H_\alpha)$ coupling which is active throughout T_{CP}. In agreement with the experimental observations shown in Figure 2, dispersion profiles predicted by numerical simulations display a small increase in R_2 as (ν_{CP} increases from 50 Hz to 400 Hz, with T_{CP} = 40 ms. Although the use of REBURP CPMG pulses overcomes this problem, experiments are limited to small effective fields, as noted above.

Another potential source of spurious R_2 dispersion is $^1H\text{-}^1H$ dipolar cross relaxation, which can cause R_2 to oscillate as ν_{CP} increases (Ishima et al., 1999; Vold and Chan, 1972). When the chemical shift difference between amide and aliphatic protons $\Delta\nu$, is much greater than ν_{CP}, transverse cross-relaxation involving these types of protons is not expected to have a large effect on the dispersion measurement (Ishima et al., 1999; Vold and Chan, 1972). For example, in the case of an amide and aliphatic proton having $\Delta\nu$ = 2 kHz and a cross relaxation rate, σ, of 6 s^{-1} (calculated for a protein with τ_C = 10 ns and r_{HH} = 2.2 Å), the amide proton transverse signal intensity changes by less than 5%, as ν_{CP} varies from 50 to 400 Hz, when T_{CP} = 40 ms. Later, when considering cross-relaxation of amide protons we discuss the more general case where $\Delta\nu$ and ν_{CP} have arbitrary values.

Although the relaxation profiles obtained using the pulse sequence of Figure 1A provide qualitative evidence for chemical exchange, it is desirable to suppress the artifacts discussed above, which is done in following manner. First, artifacts arising from $^3J(H_N\text{-}H_\alpha)$-couplings are eliminated by using a $^1H\text{-}^{15}N$ labeled protein that is perdeuterated at non-exchanging hydrogen sites. In addition to eliminating the $^3J(H_N\text{-}H_\alpha)$ coupling, perdeuteration significantly reduces proton-proton dipolar cross-relaxation. Furthermore, by reducing the number the proton dipolar interactions, perdeuteration significantly decreases the amide proton R_2 values. A further reduction in the amide proton R_2 values is achieved by modifying the sequence in Figure 1A by placing the CPMG section of the sequence after the t_1 evolution period as shown in Figure 1B. Although Rance–Kay coherence selection cannot be conveniently applied, the dipolar coupled amide protons relax as unlike spins (Ishima et al., 1998), decreasing their transverse relaxation rates. This increases signal to noise and sensitivity of R_2 to chemical exchange. In addition, placing the CPMG period after the t_1 period significantly diminishes the effect of amide cross relaxation on the HSQC signal intensities, because the HSQC signals their corresponding cross-peaks are not degenerate (unless the ^{15}N chemical shifts of the cross-relaxing amides are the same). If desired, the IPAP approach can be incorporated into the sequence to further decrease the proton R_2 and to improve resolution in the proton dimension (Ishima et al., 1998).

In general, amide-amide cross-relaxation rates are expected to be small compared with ^1H auto relaxation rates, because amide interproton distances typically exceed 2.7 Å. However, amide-amide cross relaxation may affect R_2 measurements if the chemical shift difference of the dipolar coupled amide protons is small compared with ν_{CP}. Fortunately, amide protons experiencing significant cross-relaxation can be readily identified from cross peaks observed in 2D $^1H\text{-}^{15}N$ correlated ^1H ROSEY or NOESY spectra (Ishima et al., 1998) and excluded from an analysis. Alternatively the signal intensities can be corrected as described in Supplementary material, where it is shown that cross relaxation causes a systematic increase in the fractional signal intensity of less than ca. $(\sigma T_{CP})^2/2$. At 20 °C the overall correlation time of the protease is 12.8 ns (Freedberg et al., 2002). Using this correlation time and an interproton distance of by 2.7 Å, one finds σ = 3.8, which corresponds to fractional errors in signal intensities of less than 4.6% and 1.2%, for T_{CP} = 80 ms and 40 ms, respectively. Because these errors are small we did not correct R_2 values measured herein. However, when cross relaxation is more significant, the correction described in the Supplementary material reduces the error to less than a few percent for values of σT_{CP} as large as 0.5. Provided that the precautions just discussed are followed, neither $^3J(H_N\text{-}H_\alpha)$ nor transverse cross relaxation mechanisms should introduce large errors into R_2 dispersion data.

The modified R_2 dispersion sequence (Figure 1B) was applied to a sample of perdeuterated HIV-1 protease bound to the inhibitor DMP323, a complex whose molecular mass is 22 kDa. Although the experiments were recorded at 20 °C, where τ_C = 12.8 ns (Freedberg et al., 2002), the average amide proton R_2 value was small, ca. 20 s^{-1}. As a consequence of the small ^1H R_2 values, we were able to record ^1H dispersion profiles with good sensitivity at external fields of 500 and 800 MHz. Proton R_2 values were measured at 12–14 effective fields ranging from 25 Hz to 2 kHz in 48–60 h at a protein (dimer) concentration of 0.25 mM. Because the $C_\alpha H$-sites are deuterated, modulation by $^3J(H_N\text{-}H_\alpha)$ coupling is not significant and a

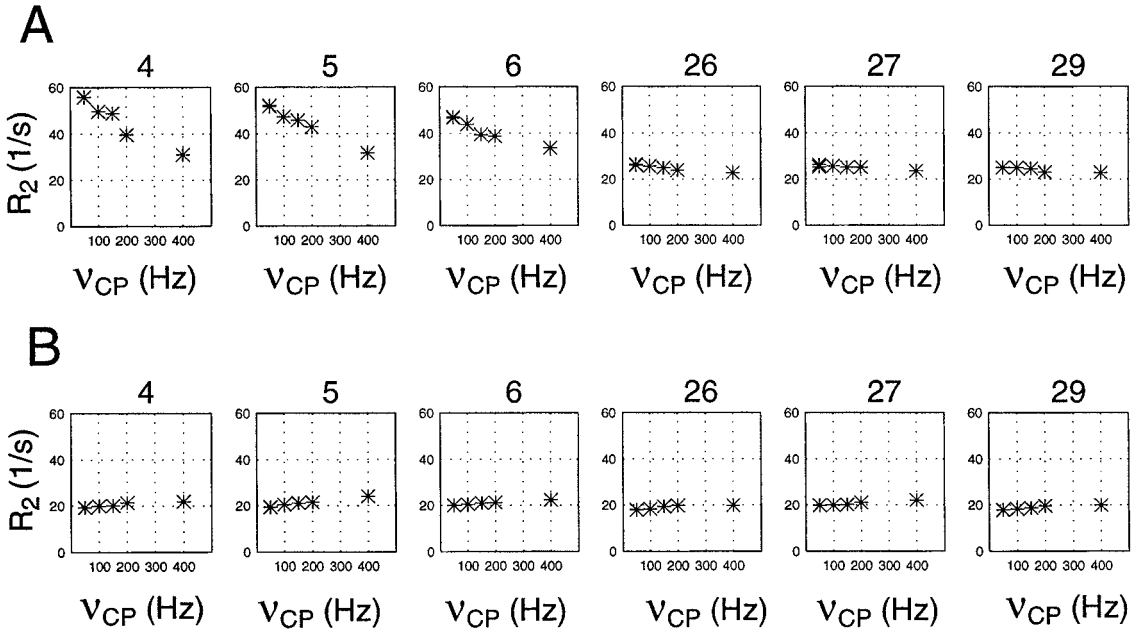

Figure 2. Comparison of proton relaxation dispersion profiles of residues of ^{15}N-labeled ubiquitin (VLI Research, Southeasten, PA) recorded using either (A) a rectangular 180° pulse or (B) a REBURP pulse, as the pulse indicated by the hatched bar in Figure 1A. Residue numbers are shown on top of each panel. In residues 4, 5 and 6, $^{3}J(H_N\text{-}H_\alpha) > 9$ Hz while in residues 26, 27 and 29, $^{3}J(H_N\text{-}H_\alpha) < 6$ Hz. The REBURP pulse eliminates most of the spurious dispersion due to $^{3}J(H_N\text{-}H_\alpha)$-coupling seen in (A). All spectra were recorded on a 1.6 mM protein sample dissolved in 95% H_2O/5% D_2O, pH 4.7.

non-selective rectangular 180° pulse can be used in the rcINEPT period if desired, in place of the REBURP pulse. The fractional error in R_2 due to random noise is given by $(\delta_e / I_0)(1+(I_0/I_{CP})^2)^{1/2}/(R_2T_{CP})$ where δ_e is the rms noise and I_0 and I_{CP} are intensities measured at time zero and at T_{CP}. Typically errors in the proton R_2 measured at 500 MHz were less than 3% for R_2 less than 20 s^{-1} and ca. 8% when R_2 was ca. 40 s^{-1}, in cases when ^{15}N chemical exchange was small, R_{ex} less than ca. 5 s^{-1}. Fractional errors increased, in accord with the above equation, in cases where signal intensity was significantly diminished because of amide ^{15}N chemical exchange.

Figure 3A displays amide proton dispersion profiles measured at 500 MHz for residues in the N-terminus of the protease. This region of the protein backbone is of functional importance, containing a labile loop that may regulate activity and an interfacial β-strand that stabilizes formation of the active protease dimer. In this experiment ν_{CP} varied from 25 Hz to 2 kHz, nearly two orders of magnitude. Our previous ^{1}H relaxation study of slow protease dynamics (Ishima et al., 1998), using two ν_{CP} values (100 and 300 Hz) and three spin lock fields (2, 4 and 6 kHz) identified R_2 dispersion for residues, 3, 4 and 6. However the R_2 dispersion seen for residues 2, 7, 8 and 10 in Figure 3A was not evident in the earlier data because the chemical exchange contribution to transverse relaxation was too small to observe when ν_{CP} > ca. 100 Hz.

The proton R_2 dispersion seen in the protease at 500 MHz is confirmed by R_2 dispersion profiles measured at 800 MHz (Figure 3B). In fact the R_2 dispersion of residues 2, 3, 7, 8 and 10 is amplified significantly at the higher field, a result that indicates that the exchange rate is outside the slow (lifetime broadening) limit. With complete dispersion profiles at two external fields it should be possible to determine the exchange correlation time (Millet et al., 2000). Although amplification of exchange effects at 800 MHz makes it possible to observe weak R_2 dispersion, when chemical exchange is strong, as it the case for residues 4 and 6, the exchange broadening is so large that the accurate signal intensities cannot be measured in the relaxation spectra. In such cases it may still be possible to make useful dispersion measurements provided that one measures R_2 using a short constant time period (<25 ms) and large ν_{CP} value (> 100 Hz), conditions which diminish signal loss due to exchange broadening but restrict R_2 measurement to rather large effective fields.

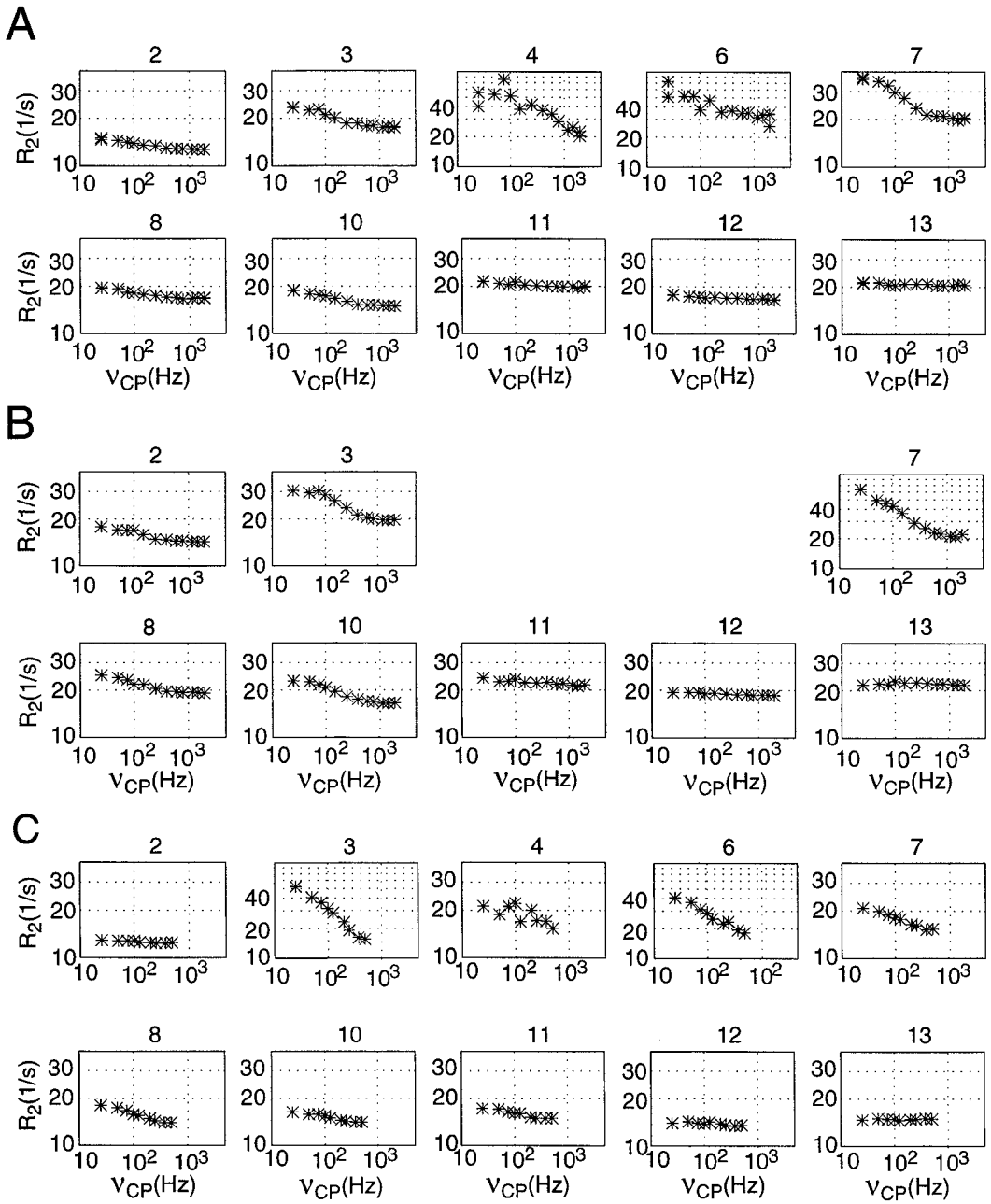

Figure 3. Comparison of ^{1}H and ^{15}N relaxation dispersion profiles of N-terminal residues of ^{15}N-labeled perdeuterated HIV-1 protease prepared as described previously (Ishima et al., 1998). All spectra were recorded using a single sample of the protein bound to the potent inhibitor DMP323, dissolved in 20mM sodium acetate buffer (pH 5.2, 95% H_2O/5% D_2O) at a concentration of 0.25 mM and 20 °C. ^{1}H experiments were recorded using (A) a 500 MHz Bruker DMX spectrometer and (B) an 800 MHz Bruker DRX spectrometer. ^{15}N experiments (C) were recorded using a 500 MHz Bruker DMX spectrometer equipped with a cryoprobe™. Residue numbers are shown on the tops of the graphs. In (B), the dispersion profiles for residues 4 and 6 were not obtained because severe exchange broadening precluded accurate measurement of signal intensities at the high external field. The proton profiles were obtained using the sequence in Figure 1B. The ^{15}N profiles were obtained using a published sequence (Tollinger et al., 2001), with minor modifications appropriate for a cryoprobe™. Note that the ^{1}H R_2 values could be measured at effective fields, ν_{CP}, over three times larger than could used for ^{15}N, because of the much larger magnetogyric ratio of the proton.

It is interesting to compare the ^{1}H relaxation dispersion profiles (Figures 3A and 3B) with those obtained for ^{15}N (Figure 3C). The latter experiments were recorded using the same deuterated sample as the former. The use of the deuterated protein decreases the R_2 of the N_xI_z coherence (which evolves during the CPMG periods) of most residues by nearly a factor of two, significantly increasing the sensitivity of the ^{15}N experiment to exchange. It is clear from the profiles shown in Figure 3C that, in agreement with the proton results, the ^{15}N measurement reveal that residues 2–11 are flexible on the ms-μs timescale. Moreover, the two experiments give more comprehensive information about protease backbone flexibility than does either alone. For example, the form of the large R_2 dispersion of residue 6 is more clearly seen in the ^{15}N profile while the reverse is true for residue 4. In the case of residues having small R_2 dispersion, the dispersion is more clearly revealed in the ^{1}H data for residue 2, but in the ^{15}N data for residue 11. Finally, a comparison of the ^{1}H and ^{15}N profiles obtained at 500 MHz, Figures 3A and 3C, reveals that the R_2 dispersions of the two spin types have similar magnitudes. This observation places restrictions on the possible mechanisms of the exchange broadening. For example, it is highly unlikely that it could be due to a fluctuation in the local magnetic field of an aromatic ring. Such a mechanism would affect the R_2 of ^{15}N much less than that of ^{1}H because of the ten-fold smaller ^{15}N magnetogyric ratio.

In comparing the relative merits of the two experiments, we note that off-resonance effects perturb ^{15}N relaxation profiles to a greater degree than ^{1}H profiles. This is the case because the chemical shifts of the two types of spins are dispersed over similar frequency ranges, but proton π pulse widths are typically four to seven-fold less than those of ^{15}N. We recorded the ^{15}N dispersion data, but not the ^{1}H data, using two different carrier frequencies in order to reduce off resonance effects. As discussed above, a disadvantage of the proton experiments is that the amide protons experience transverse cross-relaxation. However cross-relaxation effects can be minimized or corrected as described above, and R_2 dispersion profiles can be reliably measured at higher effective fields for ^{1}H than for ^{15}N, because the proton refocusing pulse widths are much shorter than those of ^{15}N. This proved useful in the present investigation because, as is seen in Figure 3, the plateau region of the dispersion profiles (which occurs when ν_{CP} > ca. 800 Hz) was attained in the ^{1}H experiments but was just beyond the upper limit ($\nu_{CP} = 600$ Hz) of the ^{15}N experiments.

Acknowledgement

This work was supported by the Intramural AIDS Targeted Anti-Viral Program of the Office of the Director of the National Institutes of Health. Supplementary material is available from the authors.

References

Carr, H.Y. and Purcell, E.M. (1954) *Phys. Rev.*, **94**, 630–638.
Freedberg, D.I., Ishima, R., Jacob, J., Wang, Y.X., Kustanovich, I., Louis, J.M. and Torchia, D.A. (2002) *Protein Sci.*, **11**, 221–232.
Geen, H. and Freeman, R. (1991) *J. Magn. Reson.*, **93**, 93–141.
Ishima, R., Louis, J.M. and Torchia, D.A. (1999) *J. Magn. Reson.*, **137**, 289–292.
Ishima, R., Wingfield, P.T., Stahl, S.J., Kaufman, J.D. and Torchia, D.A. (1998) *J. Am. Chem. Soc.*, **120**, 10534–10542.
Kay, L.E., Keifer, P. and Saarinen, T. (1992) *J. Am. Chem. Soc.*, **114**, 10663–10665.
Loria, J.P., Rance, M. and Palmer, A.G. (1999) *J. Am. Chem. Soc.*, **121**, 2331–2332.
Marion, D., Ikura, M., Tschudin, R. and Bax, A. (1989) *J. Magn. Reson.*, **85**, 393–399.
Meiboom, S. and Gill, D. (1958) *Rev. Sci. Instrum.*, **29**, 688–691.
Millet, O., Loria, J.P. and Kroenke C.D., Pons M., Palmer A.G. (2000) *J. Am. Chem. Soc.*, **122**, 2867–2877.
Mulder, F.A.A., Hon, B., Mittermaier, A., Dahlquist, F.W. and Kay, L.E. (2002) *J. Am. Chem. Soc.*, **124**, 1443–1451.
Mulder, F.A.A., Skrynnikov, N.R., Hon, B., Dahlquist, F.W. and Kay, L.E. (2001) *J. Am. Chem. Soc.*, **123**, 967–975.
Palmer, A.G., Cavanagh, J., Wright, P.E. and Rance, M. (1991) *J. Magn. Reson.* **93**, 151–170.
Palmer, A.G., Kroenke, C.D. and Loria, J.P. (2001) *Meth. Enzymol.*, **339**, 204–238.
Ross, A., Czisch, M. and King, G.C. (1997) *J. Magn. Reson.*, **124**, 355–365.
Skrynnikov, N.R., Mulder, F.A.A., Hon, B., Dahlquist, F.W. and Kay, L.E. (2001) *J. Am. Chem. Soc.*, **123**, 4556–4566.
Tollinger, M., Skrynnikov, N.R., Mulder, F.A.A., Forman-Kay, J.D. and Kay, L.E. (2001) *J. Am. Chem. Soc.*, **123**, 11341–11352.
Vold, R.L. and Chan, S.O. (1972) *J. Chem. Phys.*, **56**, 28–31.